Uncertainty Analysis of Thunderstorm Nowcasts for Utilization in Aircraft Routing

Manuela Sauer and Thomas Hauf
Institute of Meteorology and Climatology
Leibniz Universität Hannover
Hannover, Germany
Email: sauer@muk.uni-hannover.de

Caroline Forster
Institute of Physics of the Atmosphere
Deutsches Zentrum für Luft- und Raumfahrt (DLR)
Oberpfaffenhofen, Germany
Email: Caroline.Forster@dlr.de

Abstract—**Weather related uncertainty is a major disturbing factor in accurate aviation route planning. Adverse weather itself impacts the planning process but that might be mitigated if weather forecasts or nowcasts are used. Knowing that no forecast is perfect, the forecast for a certain time will always differ from the real weather at that time. Assuming that the forecast represents the best knowledge about the future development, deviations from it can be interpreted as the current inherent uncertainty of the forecast. We focus on thunderstorm nowcasts for the next hour using the DLR Rad-TRAM nowcast system. We analyse the nowcast error, respectively the increasing uncertainty with nowcast time by determining the spatial deviations of nowcast and observed thunderstorm extension. An intuitively expected increase of uncertainty with nowcast time is confirmed and quantified by the study results. A potential application of the uncertainty will be presented.**

I. Introduction

Uncertainty is a major issue in air traffic very often caused by adverse weather affecting single flights or airports. Delays of flights may accumulate and disturb the whole system. As introduced in the ComplexWorld Position Paper [2] uncertainty is defined as being a condition of limited knowledge about the current state or a future outcome. In the atmosphere some processes or at least their onset exhibit an inherent uncertainty that prevent an accurate forecast [1].

Thunderstorms formed by convection emerging from atmospheric instabilities are one of such phenomena. On a spatial scale of several kilometres the lifetime of mid-size thunderstorms is 20 minutes to one hour. The onset of convection is a stochastic event in the spatially intense varying atmosphere. A minimum distortion may lead to only fair weather clouds or even a much larger scale response which definitely has to be avoided by aircraft. The ability of weather forecast, regardless of whether it is deterministic or probabilistic (the latter are typically provided by an ensemble of slightly differing model runs) to accurately predict a potential for deep convection is limited especially due to stochastic onset of thunderstorms and their small scale characteristics.

Once the stochastic event of convection has started, the event becomes visible and its further development can be deduced based on observations. This is done by so called nowcast systems as Rad-TRAM that provide deterministic short term forecasts, so called nowcasts, for up to one or several hours.
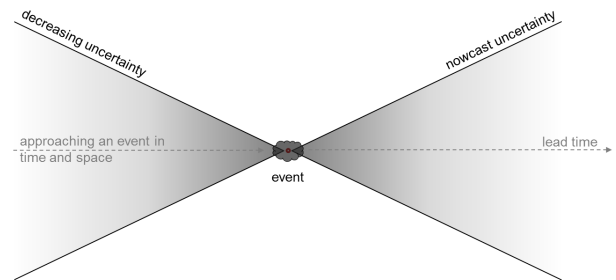

Fig. 1. Intuitive spatial uncertainty decrease when approaching an object or event in time and space and, vice versa, an opening cone of uncertainty representing the increase of the latter with growing lead time of an observation based nowcast.

When approaching the convective object in an aircraft or in the nowcast, which means the required lead time of the nowcast decreases, spatial dimensions become less uncertain up to its certain stage when it is reached in time and/or space (see closing cone in Figure 1). According to what was said before, uncertainty decreases with approaching an object or event and is, vice versa, increasing with the nowcast horizon. Starting from an observation, an opening cone of uncertainty (see Figure 1) is expected to be found when analysing uncertainty of nowcast data. The growth rate of the error made in a nowcast or forecast is said to depend on the spatial scale of the phenomena, leading to a so-called spatio-temporal chaos. In case of small scale phenomena like thunderstorms, Craig [1] states the error would double within about 30 minutes.

The objectives are to deduce an uncertainty out of a set of nowcast data and describe its development with nowcast time to enhance trajectory planning in case of adverse weather by accounting for this nowcast uncertainty. In weather avoidance modelling aircraft trajectories are often calculated around adverse weather which is represented by polygonal areas. Taking into account deterministic nowcasts of thunderstorms one might ask for probability of their occurrence as it is predicted or for uncertainty to be considered in simulations. The latter can be done by adding an uncertainty margin to the polygon as presented in Figure 2. The determination of
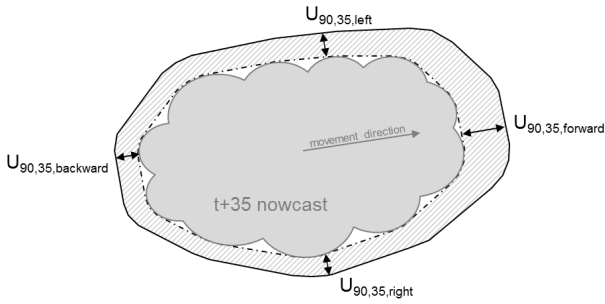
Fig. 2. Uncertainty margin (hatched area) around a nowcasted weather polygon (grey) representing, for instance, the 90th percentile of the uncertainty analysis in for directions with respect to the cells movement direction as further described in this paper.

Fig. 3. Set of nowcast data. For each observed cell (e. g. first object in bottom line) 12 nowcasts (vertical column) are provided for the next hour (timely resolution of 5 minutes). The set of nowcasts is updated when the new observations (next column) is published every 5 minutes.

this margin by quantifying the nowcast uncertainty is what is investigated in this paper.

The paper is structured as follows: Rad-TRAM data are described in Section II followed by methodological aspects in Section III. Results of the nowcast uncertainty analysis are presented in Section IV. Basics of the application of Rad-TRAM nowcasts and the identified uncertainty in the adverse weather diversion model DIVMET are given in Section V. A conclusion and a short outlook finally close the paper in Section VI.

II. RAD-TRAM DATA

Rad-TRAM (Radar Tracking and Monitoring) is a thunderstorm nowcast system developed by the German Aerospace Centre (DLR). It is based on the German radar composite (RX product) issued by the German Weather Service (DWD). The radar product gives radar reflectivities in dBZ with a horizontal resolution of $1\,km\,x\,1\,km$ as observed by precipitation radar scans at lowest elevation covering Germany [4]. An updated RX product is published every 5 minutes and serves as input for Rad-TRAM [3].

Three steps processed with the data by Rad-TRAM are detection, tracking and nowcasting. First, cells with a reflectivity higher than 37.0 dBZ, which is equivalent to moderate to heavy rain, and a size of at least three pixels are extracted and extended to at least 21 pixels by applying a circular smoothing. Second, a pixel-based motion field is determined based on radar images over the last 15 minutes. A pyramidal image matcher was developed which does not only account for the displacement but also for the growth or decay of the cells [10]. For further details on the distinct description of the procedure, please refer to Kober [11]. In the third step, the derived motion vector field is applied to the detected cells and a short range forecast is generated that provides deterministic cell contours in a spatial resolution of $2\,km\,x\,2\,km$. The nowcast product encompasses the observed cell and 12 related nowcasts for the next hour with a timely resolution of 5 minutes, which equals one column of objects given in Figure 3. Within one nowcast cycle, the former column, the cell develops and is displaced, thus a
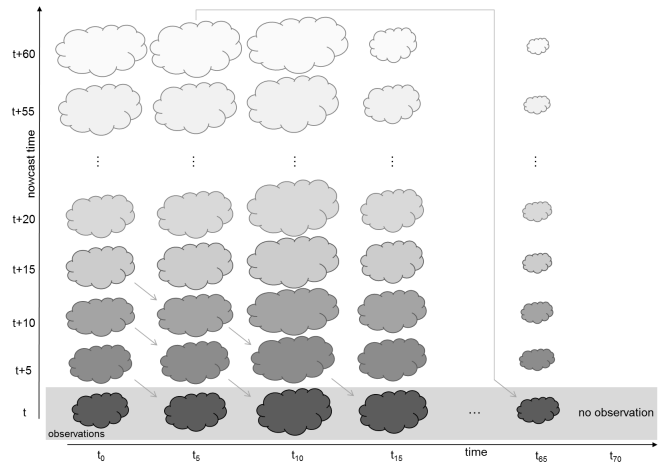
prediction of different cell stages up to 60 minutes ahead is provided. With every update of the radar product a new nowcast cycle is released for each of the observed cells according to the three step processing of the Rad-TRAM algorithm based on the WX product (next column in Figure 3).

Splitting and merging processes of cells are identified in the image matching procedure of Rad-TRAM. The system pursues the identification of the larger member of the splitting or merging process while creating a new id or discarding the one of the smaller member, respectively. Thus, the disappearance of a cell id in the data set does not necessarily mean that the cell really disappeared but it could have merged with another larger cell and is now kept with another id. Former nowcasts of both cells that merged into one, consequently exhibit a deviation in at least one direction (where the merging happened).

Validation of Rad-TRAM so far focussed on object- and pixel-based evaluations whether an event was correctly nowcasted or not. An analysis on the spatial extend and especially its error made in nowcasting convective cells has not been investigated before.

III. METHODOLOGY OF UNCERTAINTY DETERMINATION

The deterministic nowcasts of thunderstorm cells provided by Rad-TRAM are assumed to represent the best knowledge about the future development. Spatial deviations of the nowcasts to the later observations can be interpreted as the inherent uncertainty of the nowcast and a probabilistic statement can be deduced.

The uncertainty of thunderstorm nowcasts has two components: first, advection that describes the translocation of the cell and, second, its size which depends on the cells development whether it grows or shrinks.

We analyse the nowcast error, respectively the uncertainty with nowcast time by determining the spatial deviations of nowcast and observed thunderstorm extension. A 5 minutes nowcast is compared to the next observation 5 minutes ahead, the 35 minutes nowcast to the observation made 35 minutes after publication of the nowcast and so on. Depending on the age of an observed cell, respectively the number of earlier observations, there are typically several comparisons with previous nowcasts possible. Diagonally arranged nowcast cells up left to one observed cell in Figure 3 indicate comparable nowcasts. According to the limited life cycle of a thunderstorm it is not possible to find an observation to each nowcast. It might happen that there is a 60 minutes nowcast but the cell disappeared already in the meantime (i. e. after 50 minutes). Such nowcasted cells are not considered in this analysis. Thus, the uncertainty is even larger than derived here.

The spatial deviation is determined in four directions. As especially the translocation error of a nowcasted cell depends on the movement direction we apply natural coordinates adjusted to the latter of the observed cell instead of cardinal coordinates. The spatial nowcast uncertainty is then determined based on the maximum extension of nowcasted and observed cell in (forward) and against (backward) the movement direction and perpendicular to it (left and right). The relevant points are found by orthogonal projections of the object's points on the movement vector and an according perpendicular line leading through the observed object's gravity center. The distance found between two respective points (e. g. the most right points of observed and nowcasted cell) is the measure which is analysed here. As a result one will receive distance distributions separated in four directions for each nowcast time. In total 48 (= 12 x 4) distributions will emerge out of each mode of the analysis described below.

The analysis so far is processed for all 562 identified cells and their respective nowcasts on July 15th 2012; one out of 61 thunderstorm days in 2012.

A. Separated uncertainty analysis

We split the absolute uncertainty of the nowcast into translocation of the cell and development of the latter and first focussed on separated components. The idea was to identify whether Rad-TRAM systematically tends to displace the cells more to one side or faster or slower than observed.

The displacement error is determined based on the gravity centre location of both cells. Gravity centres are determined by Rad-TRAM weighted with radar reflectivities of each pixel of the cell. The dashed-dotted arrow in Figure 4 pointing from the nowcast cell's (grey contour) gravity centre to that of the observed cell (black contour) indicates the vector determined for this measure. With respect to the movement direction the displacement error vector for this example is directed back-right as will be discussed later on in Section IV-A.

The deviation of maximum extension is determined by the direction depended distance difference of each cells maximum
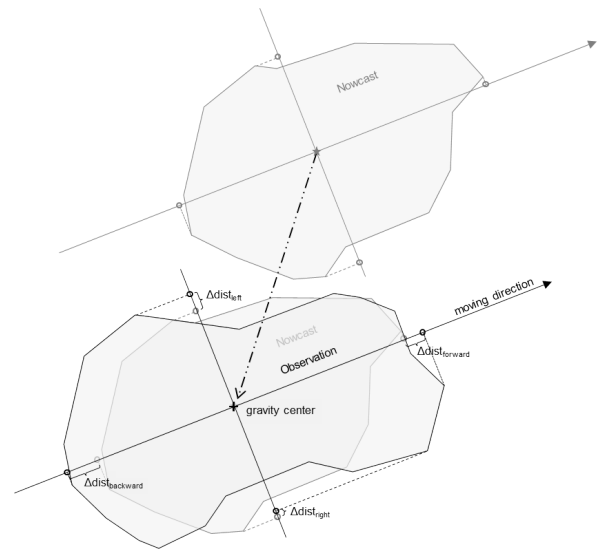

Fig. 4. Spatial uncertainty determination with separated components. The nowcasted cell is given in grey contours in the top right, the later observed cell has black contours. The error made in the nowcasted displacement is indicated by the dashed-dotted arrow directed from the nowcasted gravity centre to the observed one. Differences in size are determined by comparing each cells outer-most points, which are orthogonally projected on the movement vector or the perpendicular line, and deriving the distance between two respective points with respect to their gravity centre.

extension in all four directions with respect to its gravity centre. In other words one may overlay the nowcasted cell with the observed one so that their gravity centres are the same. The difference of maximum extension on each side, meaning the distance of respective most outer points, which are projected on the cell's movement vector for directions forward and backward and on a line perpendicular to it for the lateral directions, is the measure taken here for the spatial uncertainty in cells size. If the observed cell has a larger extension to the left (as shown in Figure 4; same in forward and backward direction) than the nowcasted one, the distance is counted positive. Is the outer most point on the projection line located on the nowcasted cell (direction right in Figure 4), the distance counts negative.

B. Absolute uncertainty analysis

In order to apply the uncertainty to nowcasted weather objects as presented in Figure 2, we have also calculated the absolute uncertainty which is comprised of the uncertainties related to displacement and growth. Here the uncertainty determination is based on the absolute deviation of both cells in each direction as shown in Figure 5. As can be easily identified when comparing Figures 4 and 5, the analysis of absolute uncertainty will lead to larger deviations as it consolidates both components of uncertainty.

IV. RESULTS

A. Results of the separated uncertainty analysis

The displacement vectors of gravity centres of nowcasted and observed cell, found in the analysis described in Section
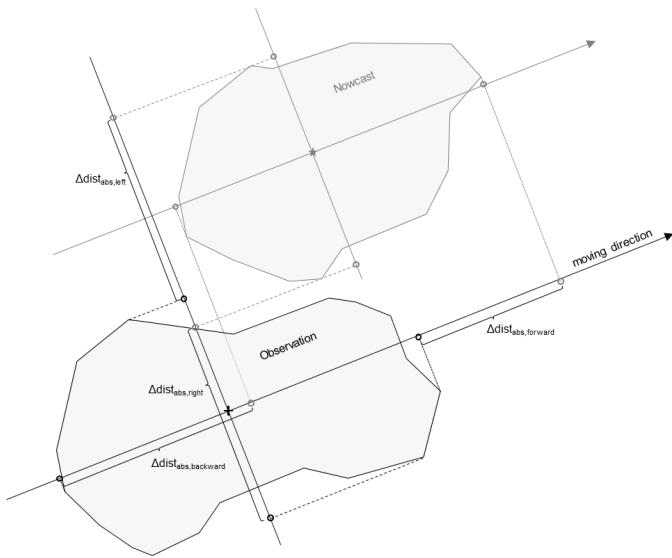
Fig. 5. Absolute spatial uncertainty determination between orthogonally projected maximum extensions of nowcasted and observed cells in four directions.
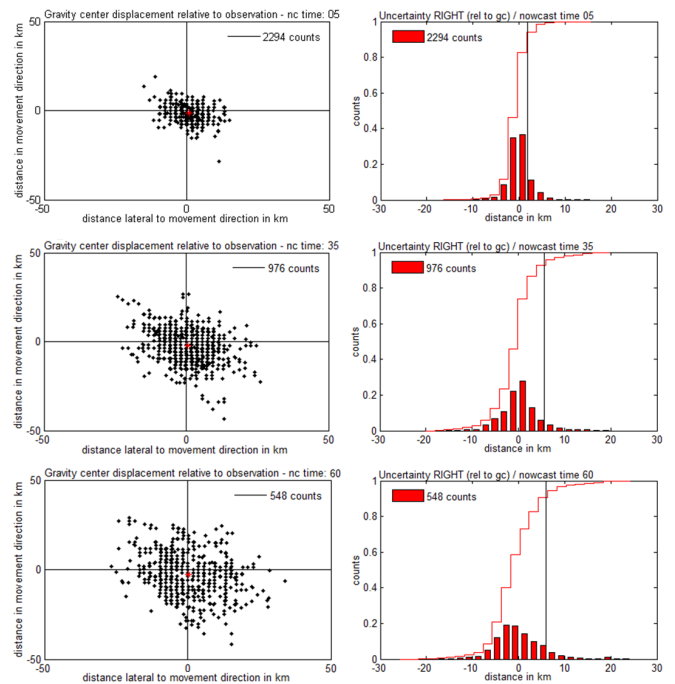

Fig. 6. Gravity centre displacement error (left panel) and spatial uncertainty in direction right of nowcasts relative to the respective gravity centre (right panel) for lead times of 5 (top), 35 (middle) and 60 (bottom) minutes.

III-A are given in the scatter plots in the left panel of Figure 6. The centre point (intersection of grid lines) of each diagram indicates the nowcasted gravity centre location. The positive ordinate represents the forward movement direction of the observed cell. Black points give the respective observed gravity centre location with respect to the movement direction. Deviations are given for 5 (top), 35 (middle) and 60 (bottom) minutes nowcasts. The displacement vector given in Figure 4 would appear here as a point in the bottom right quadrant. The red cross indicates the mean of all points but is, due to the cloud distribution around the observed gravity centre location, only slightly displaced to the latter. Therefore, a systematic displacement error of gravity centres in Rad-TRAM can not be derived from this result.

Frequency distributions of distance deviations to the right between nowcast and observation are given in the right panel of Figure 6. Positive distances describe situations in which the most right point of the observation is located right to the most right point of the nowcast, thus one will need to add a distance to the nowcast to reach the observation. In case the nowcast reaches too far to the right, the nowcast over-predicted the situation and the distance is counted negative. Histogram classes have a width of 2 km corresponding to the spatial resolution of Rad-TRAM output. The bars are normalised for better comparability, however, the number of counts decreases with increasing nowcast time. Having found 2294 5 minutes nowcasts to compare with a later observation, there were only 976 and 548 observations found for comparison with nowcasts for 35 and 60 minutes, respectively. This results from the short life character of convective cells which may have disappeared in the meantime. Additionally the cumulative distribution is plotted in red and the 90th percentile is given by the black line.

The distances found for different nowcast times result in a single peak distribution each which is more or less symmetric. Especially the distribution for 5 minutes nowcasts exhibits a positive excess kurtosis characterising the distribution as being leptokurtic. Nevertheless, goodness-of-fit tests like that of Jarque-Bera reject the null hypothesis that the distributions match the skewness and kurtosis of a normal distribution.

What is hinted here is a decrease of the kurtosis leading to a broader distribution with increasing lead time of the nowcasts. The 90th percentile which might be applicable for the uncertainty margin around a nowcasted cell shifts from 1.91 km to 5.68 km and 5.87 km in top-down direction of the given distributions.

The distributions for left, forward and backward directions exhibit a similar shape and thus are not shown here.

B. Results of the absolute uncertainty analysis

The frequency distributions found in the analysis of absolute deviations between nowcast and observation for lead times of 5, 35 and 60 minutes and directions left and right are given in Figure 7. The left panel shows the results for direction left in black bars. Whereas the distribution for 5 minutes looks pretty much like that of the analysis of relative deviations discussed in Section IV-A (single peak, symmetric), the distribution flattens and broadens much stronger in the absolute analysis shown here. The single peak character dissipates with increasing lead time and is disappeared in the distribution for 60 minutes nowcasts. The 90th percentile shifts from 1.98 km to 11.14 km and further to
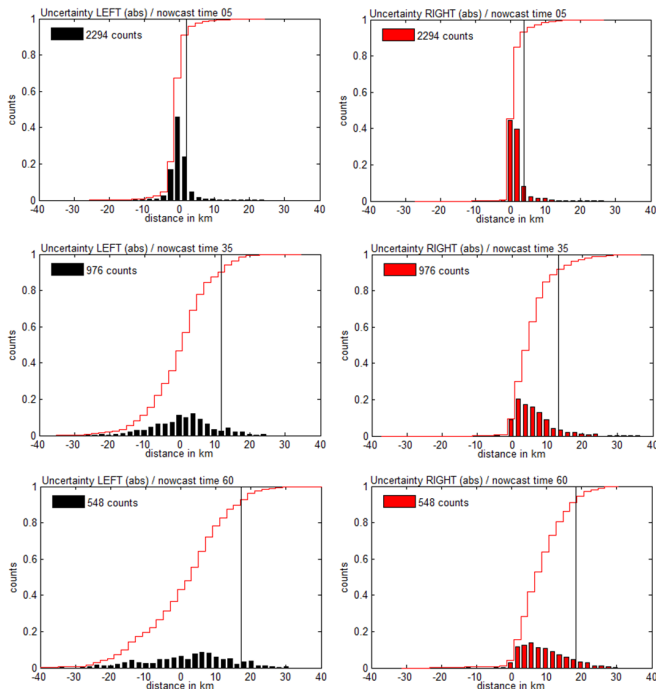
Fig. 7. Spatial deviations between nowcasted and observed cells in direction left (left panel) and right (right panel) for lead times of 5 (top), 35 (middle) and 60 (bottom) minutes.
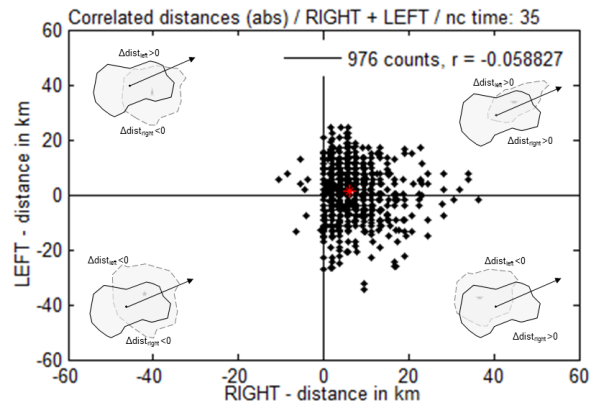

Fig. 8. Spatial absolute deviations between nowcasted and observed cells in direction left (ordinate) plotted over those in direction right (abscissa) for 35 minutes nowcasts. Small sketches in each corner indicate a sample situation of left and right deviations represented by a count in the respective quadrant. The red point indicates the gravity centre of the point cloud. The correlation coefficient r is given in the upper right corner.

17.14 km for the given lead times.

In contrast to the spatial absolute deviation distributions for direction left, those for right exhibit another shape. There is no symmetry as there are nearly no negative counts. This means that in almost all cases of July 15th, 2012 the most right point of the observed cell was more located to the right than nowcasted. Observations report on a common development of new cells at the leading right edge of existing cells in the northern hemisphere. The new cell merge the older one leading to a seemingly displacement of the cell to the right of the winds [9]. The larger number of individual thunderstorm cells are right movers, however, left movers occur occasionally. This might be due to the so called Coriolis effect that results from the Earth rotation and its ellipsoidal shape. Every long persisting movement (> 3 hours) apart the equator is influenced by the Coriolis effect and is deflected to the right in the northern hemisphere (left in the southern hemisphere). It might be that the effect of new cell formation and the resulting deflection to the right are not fully projected by Rad-TRAM as it only accounts for already existing cells. This could be a reason for the characteristic results in direction right which have to be proofed based on analyses of further thunderstorm days. Here the 90th percentile level is about 2 km larger than for direction left and shifts from 3.79 km to 13.24 km and further to 18.24 km for the given lead times.

The frequency distributions found for forward and backward direction look pretty much like those for left and thus, are not shown here.

C. Correlation between opposite direction deviations

Having analysed the deviations for each of the four directions with respect to the cells movement, one might ask about the correlation between those of opposite directions. It is expected that an object which is observed more right than nowcasted will probably not reach out of the nowcast left of the movement direction. It is rather expected that the shape and size is better nowcasted than its position. The latter might be shifted to the right or left or is displaced to slow or fast, meaning that the deviation is positive on one side and negative in the other. Scatter plots showing deviations on one of opposite directions on each axis may indicate a correlation like that discussed above, which would be given by a linear arrangement with negative slope.

A scatter plot showing absolute spatial deviations in left (ordinate) and right (abscissa) direction for 35 minutes nowcasts is given in Figure 8. Counts in the top right quadrant, for instance, reflect parameter combinations describing a situation in which the nowcast (grey contoured polygon in top right sketch) was smaller than the observed cell (black contour in same sketch) on both sides of the movement direction. The bottom right quadrant is characterised by negative distances on the left side and positive deviations on the right side, representing a situation in which the nowcast was located more left than observed later. For further explanation please see the small sketches given in each quadrant. A statement concerning forward and backward deviations are not deducible out of this chart.

The expected linear arrangement with negative slope between deviations in directions left and right, which was expected, can not be identified here. The correlation coefficient r is about zero, confirming that there is no linear correlation found. This is mainly due to the fact, that nearly no negative counts were found for direction right (see right panel in Fig. 7) while deviations to the left were positive as well as negative. Taking a look on the correlated absolute deviations in forward
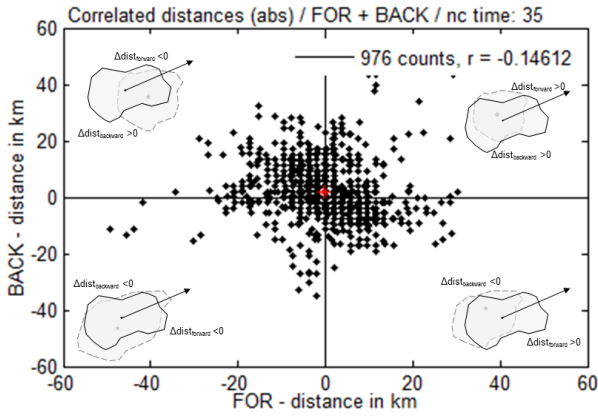
Fig. 9. Same as in Figure 8 but for forward (abscissa) and backward (ordinate) direction.
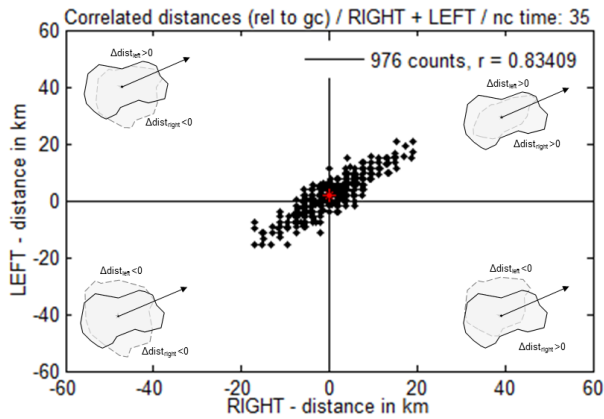

Fig. 10. Same as in Figure 8 but for deviations relative to the gravity centre of the observed cell. Nowcast and observation were overlaid for this analysis (see Section III-A).

and backward direction for 35 minutes nowcasts (Figure 9), which are roughly distributed as the ones in direction left each, one may identify a slight tendency to the expected correlation. The correlation coefficient r results in about -0.15 for the shown parameter combination. The negative correlation even intensifies with nowcast time resulting in $r = -0.56$ for 60 minutes lead time. Counts in the upper left quadrant here represent situations in which the leading as well as the back-most point of the cell were nowcasted too far ahead compared to the later observation. Thus, a tendency to rather shifted cells parallel to the movement direction is found.

Plotting the deviations found for left and right in the separated analysis (Figure 10), in which the maximum extension of one direction with respect to the related cells gravity centre were compared between nowcast and observation, the correlation looks quite different to that of absolute deviations. Now we find a strong positive linear correlation ($r = 0.83$), meaning that the cell was either predicted too small or broad on both sides simultaneously.

As there is no characteristic correlation found for spatial

deviations in different directions we still suggest to use a quantile, e. g. the 90th percentile, for consideration in weather avoidance modelling. How to regard for nowcast data and their respective uncertainty is described in the following.

V. APPLICATION OF NOWCAST DATA AND IDENTIFIED NOWCAST UNCERTAINTIES IN ADVERSE WEATHER AVOIDANCE MODELLING

The adverse weather avoidance model DIVMET, developed by Hauf *et al.* [6], allows for integration of object based nowcast data like that provided by Rad-TRAM. In DIVMET as well as elsewhere in [8], adverse weather is generally represented by polygonal areas, referred to as "no-go" zones. To account for a safety distance following international regulations, for instance given by NATS [12], weather polygons are, so far, enlarged by certain constant safety margins in DIVMET.

When accounting for nowcast data a selection of the appropriate nowcast to an observed cell is the first step to be processed. In DIVMET the selection is based on flight time distances between the current aircraft position and the respective nowcasted cell. If there are 37 minutes left to reach the nowcasted cell, the 35 minutes nowcast of the cell will be picked out of the data set. This selection is done separately for each cell. Thus, the resulting weather situation considered in the simulation of weather avoidance routing is compounded of cells with different validity times. It does not reflect one observable situation.

Having determined the uncertainty of the nowcast data as described in Sections III and IV we can now answer the earlier placed question on the timely development of uncertainty and quantities of the uncertainty cone presented in Figure 1. The 90th and 95th percentiles of deviations found in the absolute uncertainty analysis for directions left and right are given in Figure 11 by circles and stars, respectively. Each pair of same percentiles forms a cone with a certain width in kilometre (ordinate, centred at zero but running positive in both directions) for different nowcast times (abscissa). The higher the certainty of avoidance, the larger is the width of the cone (compare 90th and 95th percentiles).
The development of the uncertainty is derived from polynomial regression in a least squares sense resulting in a polynomial for each of the given uncertainty measures $u_{percentile,direction}$ which are

$$u_{90,\text{left}}(t) = -0.0023 \cdot t^2 + 0.4275 \cdot t - 0.0921$$
$$u_{90,\text{right}}(t) = -0.0021 \cdot t^2 + 0.3908 \cdot t + 2.1487$$
$$u_{95,\text{left}}(t) = -0.0029 \cdot t^2 + 0.4784 \cdot t + 2.4620$$
$$u_{95,\text{right}}(t) = -0.0039 \cdot t^2 + 0.5162 \cdot t + 4.0876.$$

Assuming an aircraft flying behind the cell in the same direction as the latter moves, the width of the cone on each side represents the distance that should be added to a nowcasted cell on the respective side in order to avoid it by 90 % certainty. In order to do so an additional margin of about 11.75 km and 13.24 km to the left and right, respectively, with
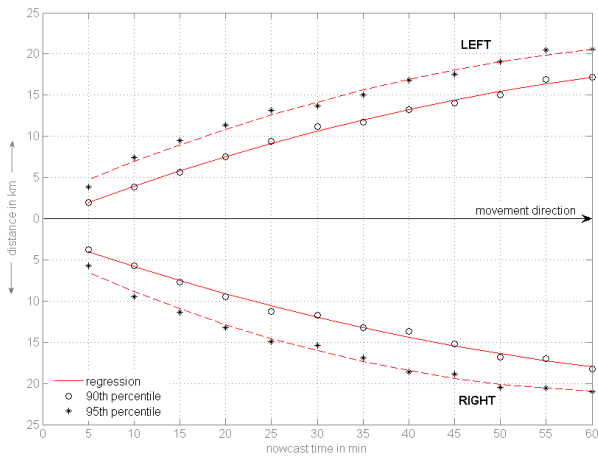
Fig. 11. Development of the 90th (circles) and 95th (stars) percentile of spatial uncertainty to the left and right of the cells movement direction in the nowcast horizon of one hour. Polynomial regression for each set is given in red lines (solid for 90th and dashed for 95th percentile).

respect to the movement direction should be added around a 35 minutes nowcast. To avoid the cell by 95 % certainty one would need to add 15.06 km and 16.90 km in the same manner. Additionally, margins in forward and backward direction (e. g. 9.71 km and 15.05 km, respectively for 90 % avoidance certainty) should be considered (not shown here). Thus, the uncertainty margin added around nowcasts is not constant but depends on the direction and nowcast time.

Whether it is worth to account additionally for a safety margin stays unanswered here. The consideration of uncertainty margins plus safety margins could result in a merging of single cells and margins around to large fields declared as being nogo zones however the actual cells are small in size. Gaps for flying through the adverse weather field actually exist but will be ignored because of the uncertainty consideration. Further studies will have a look on this issue.

VI. CONCLUSION

The research presented in this paper focussed on an uncertainty analysis of deterministic thunderstorm nowcast data provided by DLR's Rad-TRAM. Motivation leading to this analysis came along with weather avoidance modelling, the integration of nowcast data and the rising demand of probabilistic statements in the ATM society.

562 different cells were identified by Rad-TRAM in radar data of July 15th, 2012. For each cell's observation a cycle of 12 nowcasts covering the next hour with a timely resolution of 5 minutes is provided by Rad-TRAM. The uncertainty analysis presented here is based on spatial deviations of maximum extension between nowcasts and the related later observation of a cell in and against the cell's movement direction and lateral to it. Nowcast uncertainty origins of two components: advection and cell development, which are analysed separately as well as combined in an absolute deviation determination. An analysis, as presented here, has

not been performed with outputs of Rad-TRAM before and thus was reasonable as it, among the target followed here, particularly evaluates the model and provides information for its developers.

The key output here is a quantified uncertainty that enables probabilistic statements by enlarging a nowcasted cell by an uncertainty margin, which is direction dependent and e. g. ranges between 9.7 km and about 15 km for a 35 minutes nowcast when accounting for 90 % certainty to avoid the adverse weather region. Quantiles for each direction were derived from frequency distributions of absolute distances between the respective (e. g. most right points of) nowcast and observation found in each of the four directions and split for the 12 nowcast times. The increase of uncertainty within the nowcast horizon of one hour is exemplary shown for the 90th and 95th percentiles for directions left and right in Figure 11. A mathematical description of the uncertainty development is additionally derived from polynomial regression in a least squares sense forming a second degree polynomial.

To reach the same probability (90 %) of cell avoidance, one would need to add up to 17.38 km (backward direction) more to the 60 minutes nowcast of a cell than only 3.79 km on its 5 minutes nowcast (not visually shown here). As the given percentiles for directions right result in larger distance values, we can state that Rad-TRAM seems to underestimate the rightward displacement or growth of cells. By contrast, the forward displacement of the backmost point of a cell is overestimated by Rad-TRAM (not shown).

The underestimated rightward displacement is also indicated by another noticeable result. The frequency distributions found for deviations right of the cell's movement direction exhibit almost entirely positive values which signify that the observed cell is located more to right than nowcasted in almost all situations of the data set. In contrast, the distance distributions found for the remaining directions are about symmetric. Correlated deviations for opposite directions indicate a slight negative correlation for forward and backward extensions of a cell, meaning that the compared cells are rather shifted either forward or backward against each other instead of one cell (nowcast or observation) being longer in both directions. For directions left and right no correlation was found because of the previously discussed right side characteristic.

Further symmetric distance distributions for all four directions were found in the analysis on the maximum spatial extension relative to the cells gravity centre as part of the analysis of separated uncertainty. Here the distributions exhibit a single peak and have a smaller width compared to the absolute distances, thus resulting in smaller values for the determined quantiles. A correlation analysis of deviations found to the left and right of the movement direction resulted in a positive linear correlation indicating that the error made in the nowcast was about symmetric, meaning that one of the compared cells was either smaller or larger on both sides.

The displacement error analysed separately in that part shows no characteristic appearance. Instead, the misplacement of the nowcasted cell's gravity centre is about homogeneously distributed around the one of the observed cell with increasing distance range with lead time.

In order to confirm the uncertainty found and to identify characteristic uncertainties of nowcast information in different weather conditions, the analysis will be extended to several thunderstorm days in 2012. Differences of the nowcast ability may appear between convective situations embedded in frontal systems and fair weather convection, which especially differ in their movement characteristics with the former being translocated faster than the latter.

Furthermore, for utilization of the quantified uncertainty in DIVMET variable margins around an object need to be calculated and the appropriate determination of nowcasts and related uncertainty in the model must be enhanced.

REFERENCES

[1] G. C. Craig, *Probabilistic Weather Forecasting.* – In: Atmospheric Physics, Research Topics in Aerospace. U. Schumann, edt. DLR, Springer, 2012, pp. 661673.

[2] ComplexWorld Network, *ComplexWorld Position Paper.* http://complexworld.eu/wiki/ComplexWorld_Position_Paper, n.y., last accessed: 15.09.2014.

[3] DLR, *DLR Rad-TRAM (Radar Tracking and Monitoring)*, Description. n.y.

[4] DWD, *DWD Weather Radar Network.* http://www.dwd.de/bvbw/generator/DWDWWW/Content/Forschung/FE1/Datenassimilation/Radarbroschuere__en,templateId=raw,property=publicationFile.pdf/Radarbroschuere_en.pdf, n.y., last accessed: 27.08.2014.

[5] C. Forster and A. Tafferner, *Nowcasting Thunderstorms for Munich Airport.* – In: The DLR Project Wetter und Fliegen. T. Gerz and C. Schwarz, edt. Deutsches Zentrum für Luft- und Raumfahrt, 2012, pp. 3245.

[6] T. Hauf, L. Sakiew and M. Sauer, *Adverse weather diversion model DIVMET.* Journal of Aerospace Operations, Vol. 2, 2013, pp. 115-133.

[7] I.T. Jolliffe and D.B. Stephenson, *Forecast Verification: A Practitioner's Guide in Atmospheric Science.* Wiley, 2003.

[8] M. Kamgarpour, V. Dadok and C. Tomlin, *Trajectory generation for aircraft subject to dynamic weather uncertainty.* 49th IEEE Conference on Decision and Control, Atlanta, Georgia, 2010.

[9] K. A. Browning, *Morphology and Classification of Middle-Latitude Thunderstorms.* – In: Thunderstorm Morphology and Dynamics. E. Kessler, edt. Volume 2 of *Thunderstorms: A Social, Scientific, and Technological Documentary*, University of Oklahoma Press, Norman, 2. Edition, 1986, pp. 133-152.

[10] K. Kober and A. Tafferner, *Tracking and nowcasting of convective cells using remote sensing data from radar and satellite.* – In: The DLR Project Wetter und Fliegen. T. Gerz and C. Schwarz, edt. Meteorologische Zeitschrift, Vol.1, No. 18, 2009, pp. 7584.

[11] K. Kober, *Probabilistic forecasting of convective precipitation by combining a nowcasting method with several interpretations of a high resolution ensemble.* Dissertation, Munich, 2010.

[12] NATS, *The effect of thunderstorms and associated turbulence on aircraft operations*, 3rd ed. Technical Note AIC: P 056/2010, Hounslow, Middlesex, UK Aeronautical Information Service, 2010, p. 10.

[13] D. Stich, *Convection Initiation Detection and Nowcasting with multiple data sources.* Dissertation, Munich, 2012.